

Supporting Information

Unveiling the charge storage mechanisms of Co-based perovskite fluoride in mild aqueous electrolyte

Yuzhen Zhang[†], Miao Liu[†], Rui Ding*, Yi Li, Jian Guo, Qi Fang, Miao Yan, Jinmei Xie

Key Laboratory of Environmentally Friendly Chemistry and Applications of Ministry of Education, College of Chemistry, Xiangtan University, Xiangtan, Hunan 411105, P.R. China.

*Corresponding author: Rui Ding.

*E-mail: drm8122@xtu.edu.cn; drm8122@163.com

[†]Note: Yuzhen Zhang and Miao Liu equally contribute to the work.

Table of contents	
Experimental section	
Section 1.	Synthesis of materials
Section 2.	Characterizations
Section 3.	Electrochemical measurements
Section 4.	Calculations for m_-/m_+ , Q_m , E_m , P_m .
Section 5.	The calculations of diffusion coefficients.
Section 6.	EQCM Investigations
Supplemental figures	
Figure S1.	XRD patterns of as-synthesized KCoF_3 in this work.
Figure S2.	(a) Crystal microstructure of perovskite fluorides KCoF_3 and (b) crystalline parameters of standard KCoF_3 .
Figure S3.	(a, b) SEM, (c, d) TEM images of KCoF_3 sample.
Figure S4.	EDS of KCoF_3 sample.
Figure S5.	The first four CV curves at 10 mV s^{-1} .
Figure S6.	(a) CV curves at $2 \sim 160 \text{ mV s}^{-1}$, (b) GCD curves at different current densities of the nickel foam (NF) electrode in $1 \text{ M Na}_2\text{SO}_4$ electrolyte. (c) comparison of CV (10 mV s^{-1}) and (d) GCD (1 A g^{-1}) for KCoF_3 and NF electrodes.
Figure S7.	Ex situ FTIR spectrum graphs of the KCoF_3 electrode in pristine state and assigned charge/discharge states during the first CV cycle at 10 mV s^{-1} .
Figure S8.	Ex situ Raman spectrum graphs of the KCoF_3 electrode in pristine state and assigned specific charge/discharge states during the first CV cycle at 10 mV s^{-1} .
Figure S9.	Ex situ TEM images of KCoF_3 electrode (a, b) in charging to 1.25 V state, (c, d) in discharging to -1.1 V state of the first CV cycle at 10 mV s^{-1} .

Figure S10.

(a) CV curves for the first five cycles, (b) Raw EQCM data of the KCoF_3 electrode in 1 M Na_2SO_4 electrolyte (tested in the EQCM equipment).

Figure S11.

Aqueous ECs with positive and negative mass ratios of 1-1, 1-2, 1-3 (a, c, e) CV plots at $10\sim 160\text{ mV s}^{-1}$, (b, d, f) GCD curves at different current densities.

Figure S12.

Aqueous ECs with positive and negative mass ratios of 2-1, 3-1, 4-1 (a, c, e) CV plots at $10\sim 160\text{ mV s}^{-1}$, (b, d, f) GCD curves at different current densities.

Figure S13.

(a) Ragone plot (The detailed drawing for aqueous ECs structure), (b) cycling stability of aqueous ECs in different proportions.

Supplemental tables

Table S1.

Materials / Chemicals used in this work.

Table S2.

The EIS parameters before and after cycling for KCoF_3 electrode.

Table S3.

The crystalline parameters of the newly-formed phases in the fully charged and discharged states of KCoF_3 electrode.

Supplemental references

Experimental section

Section 1. Synthesis of materials

AR or GR grade chemicals were used directly in the synthesis (Table S1). The KCoF₃ sample was prepared by a simple one-pot solvothermal method. The processes are as follows: i) Add 2 mmol CoCl₂·6H₂O, 5 mmol KF·2H₂O and 0.2 g PVP-K30 were into 36 ml ethylene glycol (EG) solvents; ii) the mixture was magnetically stirred and dispersed in an ultrasonic bath at 100 W for 30 minutes; iii) the mixture was transferred into a 50 mL Teflon-lined stainless steel autoclave, which was heated at 180°C for 6 h in an electric oven; iv) After cooling down to room temperature, the precipitates were collected by centrifugal filtration along with washing with absolute alcohol for several times, and finally dried at 95°C overnight to obtain the ultimate products.

Section 2. Characterizations

The phase property and crystal structure were checked by X-ray diffraction (XRD). X-ray photoelectron spectra (XPS), Fourier transform infrared spectroscopy (FT-IR), and Raman spectroscopy (RS) were used to investigate the surface compositions, chemical bonding and electronic structure. The morphology and size of particles are analyzed by scanning electron microscopy (SEM) and transmission electron microscopy (TEM). The crystalline microstructures are resolved by the high-resolution TEM (HRTEM) and selected area electron diffraction (SAED). The element composition and distribution were measured by the X-ray energy dispersive spectroscopy (EDS), inductively coupled plasma atomic emission spectrometry (ICP-OES) and mapping. The specific surface area, pore volume and size distribution are examined by nitrogen sorption isothermals with Brunauer-Emmett-Teller (BET) and Barrett-Joyner-Halenda (BJH) methods.

Section 3. Electrochemical measurements

The electrodes were prepared by pressing the well-mixed slurry into the nickel foam (NF) current collector followed by thorough drying at 95 °C for 12 h in an air atmosphere. The slurry was made up of specific active materials KCF, acetylene black (AB) conductive agent and polyvinylidene difluoride (PVDF) binder in a weight ratio of 7/2/1 (dissolved in N-methyl-2-pyrrolidone (NMP)). The size of the electrode sheet is $0.5 \times 1.0 \text{ cm}^2$, the active mass loading was about $3.5\text{-}4.0 \text{ mg cm}^{-2}$. The electrochemical tests were carried out by electrochemical impedance spectroscopy (EIS), cyclic voltammetry (CV) and galvanostatic charge-discharge (GCD) with a CHI660E electrochemical workstation and Neware-CT-4008 testers. The single electrodes were tested using a three-electrode system, with the target material under study (NF coated with an active substance) as working electrode (WE), a Pt sheet was employed as counter electrode (CE), and Ag/AgCl (Satd. KCl) as reference electrode (RE). The tests for the AC//KCF ASCs were conducted in an unicell with the commercial AC as the anode and KCF as cathode. The electrolytes in all tests were 1 M Na_2SO_4 aqueous solutions at room temperature.

Section 4. calculations for m/m_+ , Q_m , E_m , P_m .

For ECs, a typical two-electrode cell was used. The mass ratios of positive and negative active materials was calculated based on the charge-balance ($Q_+ = Q_-$), as shown in Eq. (1). The values of specific capacity (Q_m , C g^{-1}) for electrodes/full cells, energy density (E_m , Wh kg^{-1})/power density (P_m , kW kg^{-1}) for full cells were calculated according to the Eqs. (1)-(4).

$$m(+)/m(-) = Q_m(-)/Q_m(+) \quad (1)$$

$$Q_m = It/m \quad (2)$$

$$E_m = (Q_m \Delta V)/7.2 \quad (3)$$

$$P_m = 3.6 E_m/t_d \quad (4)$$

Where m , Q_m , ΔV , and t_d refer to the mass of active materials (g, for single electrodes, it indicates the mass of anode or cathode materials; for full cells, it means the masses of active materials of both anode and cathode), specific charge or discharge quantity ($C\ g^{-1}$, for anode, it means the charge quantity; for cathode and full-cells, it refers to the discharge quantity), voltage window (V, for ECs, two stages of voltage windows were used according to the knee points of discharging branches of GCD plots), and discharging time (s), respectively.

Section 5. The calculations of diffusion coefficients.

The diffusion coefficients were acquired by Galvanostatic Intermittent Titration Technique (GITT). The calculation method is based on the following equation (5):

$$D^{GITT} = \frac{4}{\pi\tau} \left(\frac{m_B V_M}{M_B S} \right)^2 \left(\frac{\Delta E_S}{\Delta E_\tau} \right)^2 \quad (5)$$

where τ represents the constant current pulse time, m_B , V_M and M_B are the mass loading, the molar volume, and the molar mass of the electrode material, respectively. S is the area of the electrode electrolyte interface, ΔE_S is the change of steady-state voltage during a single-step GITT experiment, and ΔE_τ stands for the total change of cell voltage during a constant current pulse τ of a single-step GITT experiment regardless of the IR-drop.¹

Section 6. EQCM Investigations

A CHI400C electrochemical workstation (Shanghai, China) equipped with a quartz crystal microbalance was used to simultaneously collect CV and EQCM data. In-situ electrochemical measurements were performed using KCoF₃ coated quartz as the working electrode, Pt foil as the counter electrode, and Ag/AgCl (Satd. KCl) electrode as the reference electrode, and 1 M Na₂SO₄ as the electrolytes. The KCoF₃ coated quartz electrodes were prepared by dispersing KCoF₃ (14 mg), AB (4 mg) and PVDF (2 mg) in 11 drops of NMP followed by ultrasonication for 30 mins to form homogeneous suspensions, then transfer 4.4 μ L of suspension to the surface of the

quartz wafer and dry at 35 °C to volatilize the solvent. The CV measurements of the KCoF₃ coated quartz electrode were performed in a constant sweep rate with simultaneous collection of the resonance frequency. The EQCM data for frequency change Δf of the crystal and mass changes (Δm) correspond the Sauerbrey equation:²

$$\Delta m = -\frac{A\sqrt{\mu_q\rho_q}}{2f_0^2} \cdot \Delta f = -C_f \cdot \Delta f \quad (6)$$

where f_0 is the resonant frequency of the crystal (7.995 MHz), A is an area of the Au disk coated on the crystal (0.196 cm²), μ_q is the AT-cut quartz constant (2.947×10¹¹ g cm⁻¹ s⁻¹), ρ_q is the density of the crystal (2.684 g cm⁻³). So the sensitivity factor of the quartz crystal C_f was 6.9 ng Hz⁻¹ cm⁻². Here, the molar weight of the carrier can be calculated according to the following equation:³

$$M_w = \frac{\Delta m nF}{\Delta Q} = \frac{C_f(-\Delta f)nf}{\Delta Q} \quad (7)$$

Where F is the Faraday constant (96500 C mol⁻¹), n is the valence number of the ion ($n = 1$ for Na₂SO₄ electrolyte), ΔQ is the charge passed through the electrode (C).

Supplemental figures

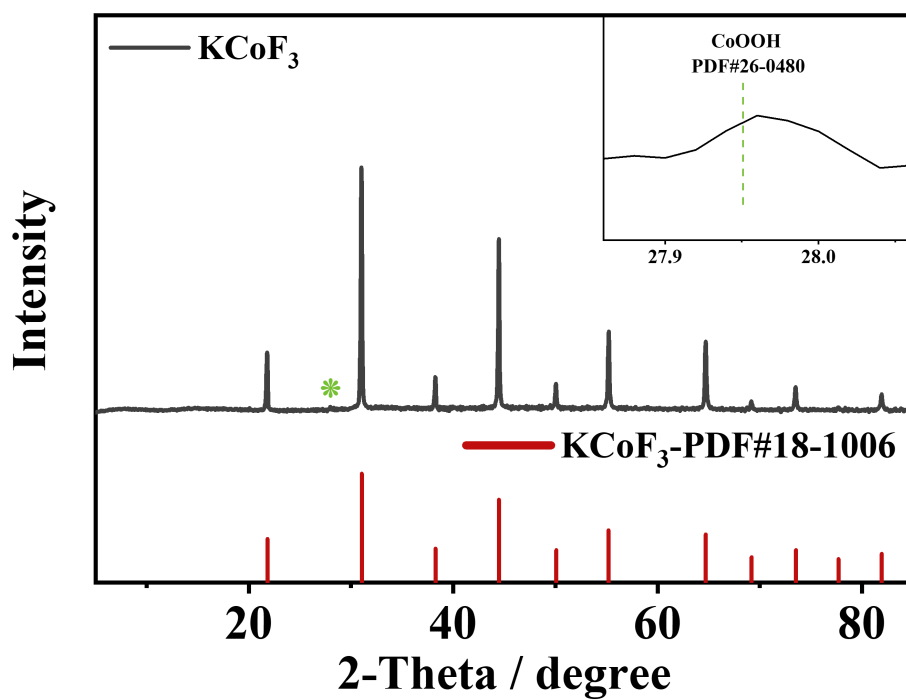


Figure S1. XRD patterns of as-synthesized KCoF_3 in this work.

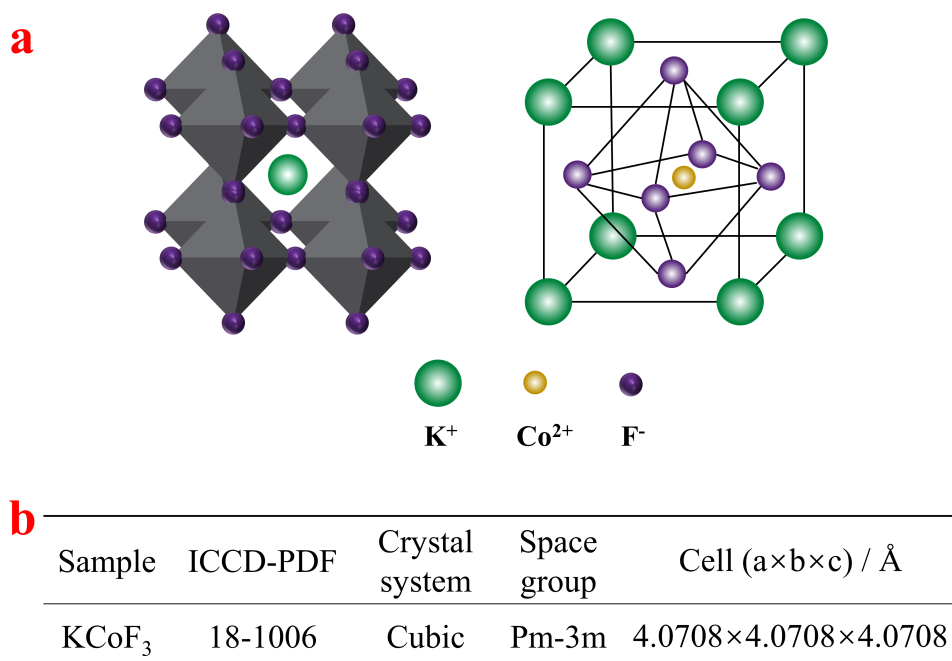


Figure S2. (a) Crystal microstructure of perovskite fluorides KCoF_3 and (b) crystalline parameters of standard KCoF_3 .

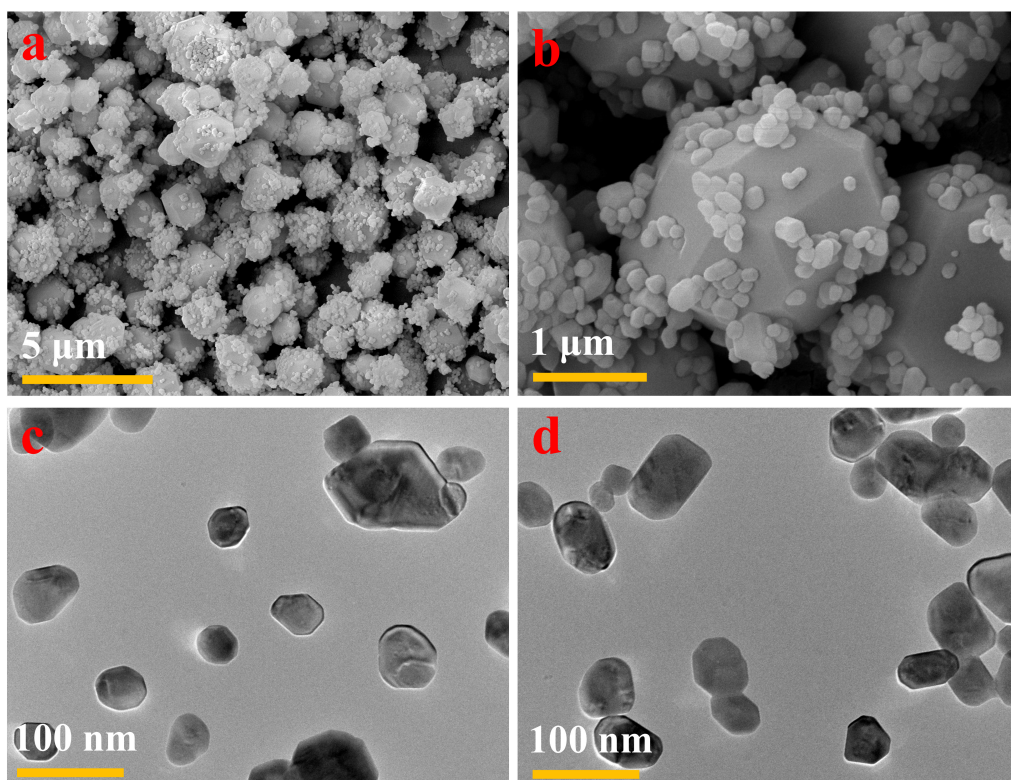


Figure S3. (a, b) SEM, (c, d) TEM images of KCoF_3 sample.

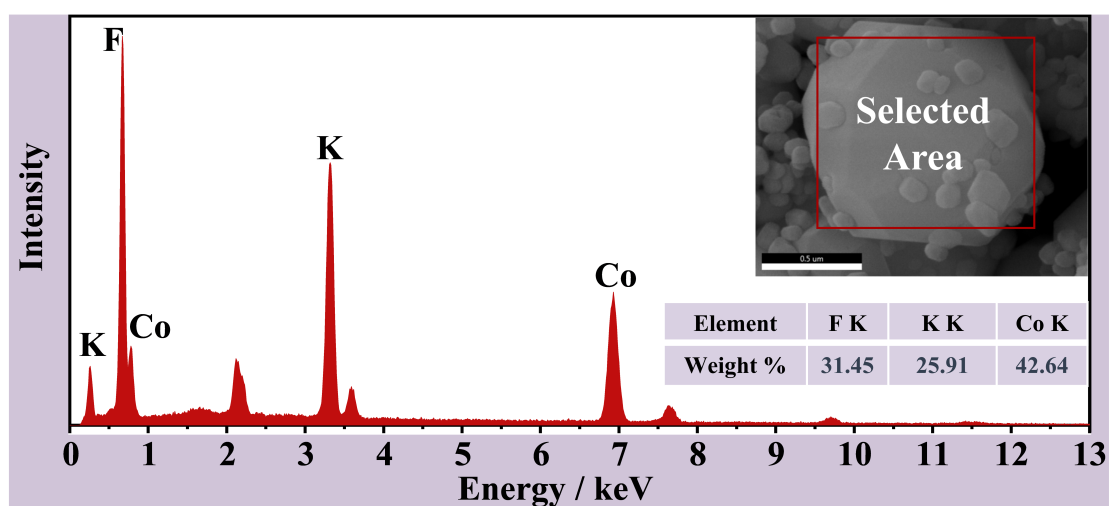


Figure S4. EDS of KCoF_3 sample.

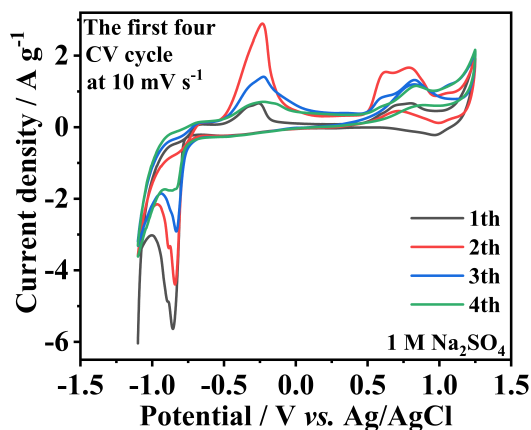


Figure S5. The first four CV curves at 10 mV s^{-1} .

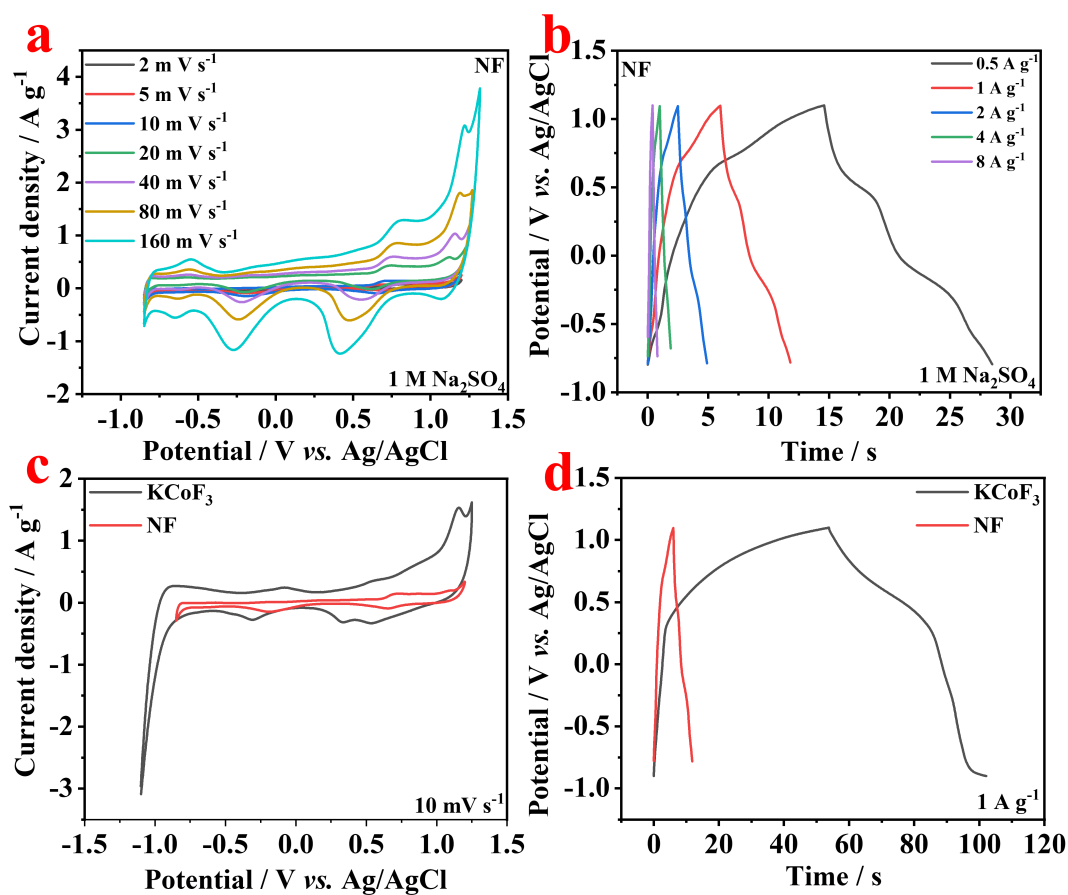


Figure S6. (a) CV curves at 2~160 mV s^{-1} , (b) GCD curves at different current densities of the nickel foma (NF) electrode in 1 M Na₂SO₄ electrolyte. (c) comparison of CV (10 mV s^{-1}) and (d) GCD (1 A g^{-1}) for KCoF₃ and NF electrodes.

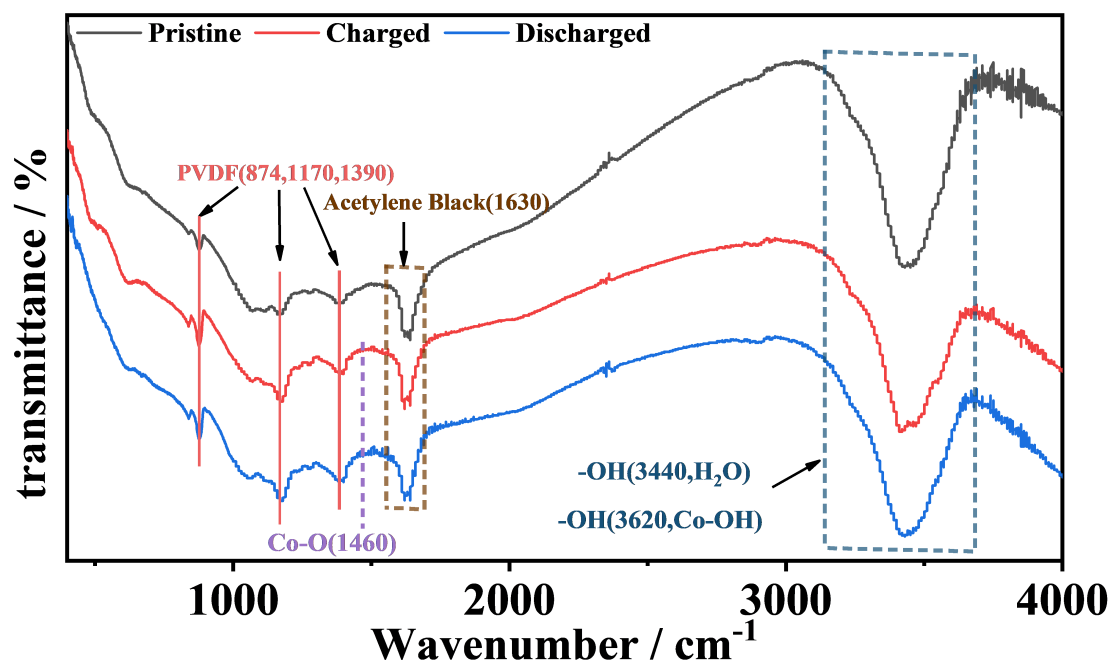


Figure S7. Ex situ FTIR spectrum graphs of the KCoF₃ electrode in pristine state and assigned charge/discharge states during the first CV cycle at 10 mV s⁻¹.

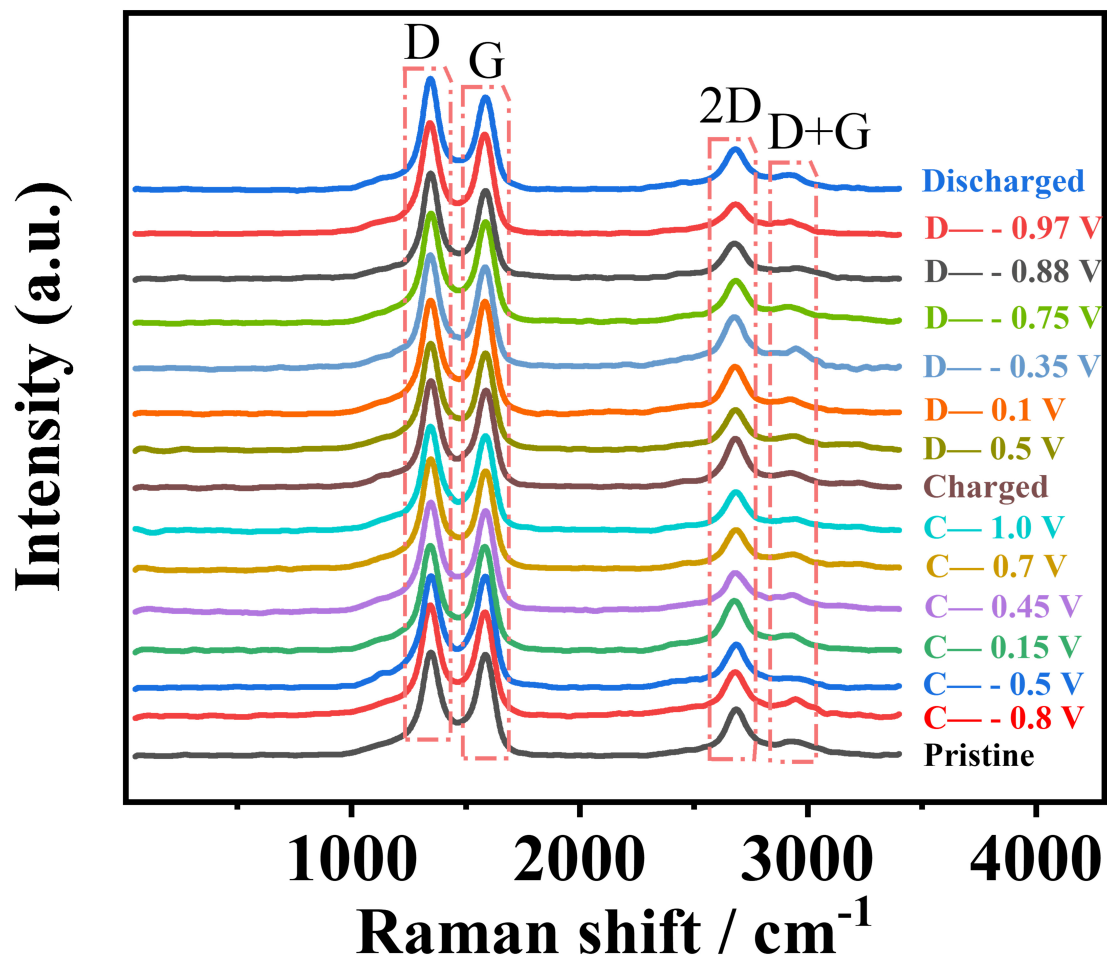


Figure S8. Ex situ Raman spectrum graphs of the KCoF₃ electrode in pristine state and assigned specific charge/discharge states during the first CV cycle at 10 mV s⁻¹.

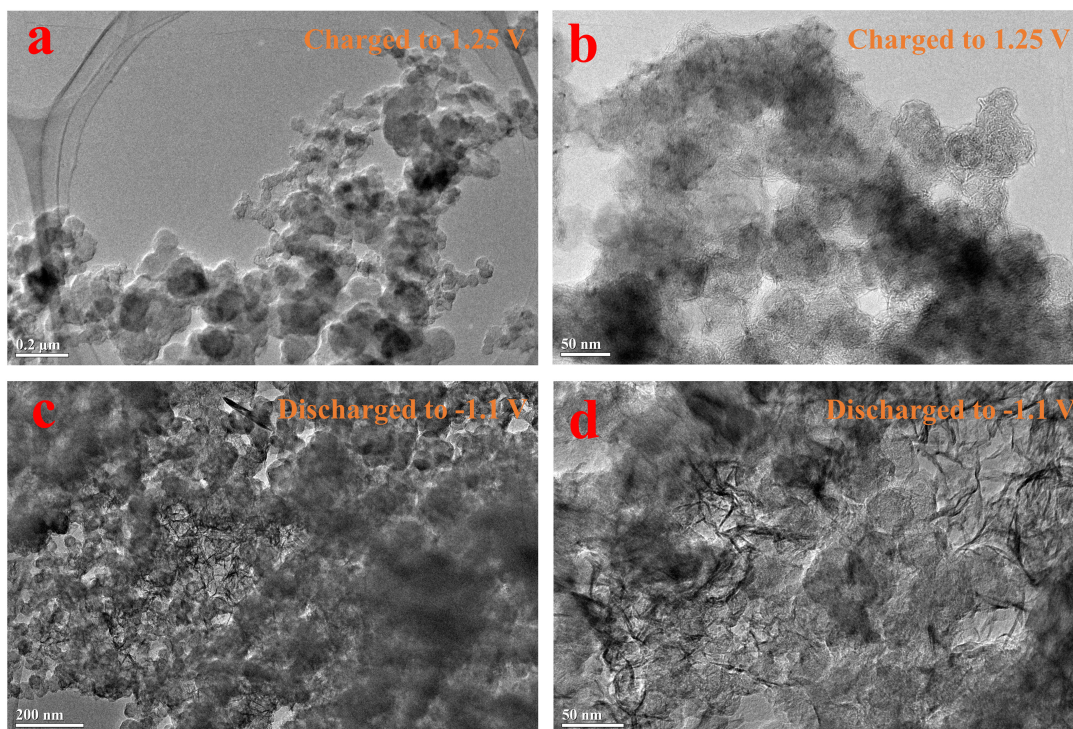


Figure S9. Ex situ TEM images of KCoF₃ electrode (a, b) in charging to 1.25 V state, (c, d) in discharging to -1.1 V state of the first CV cycle at 10 mV s⁻¹.

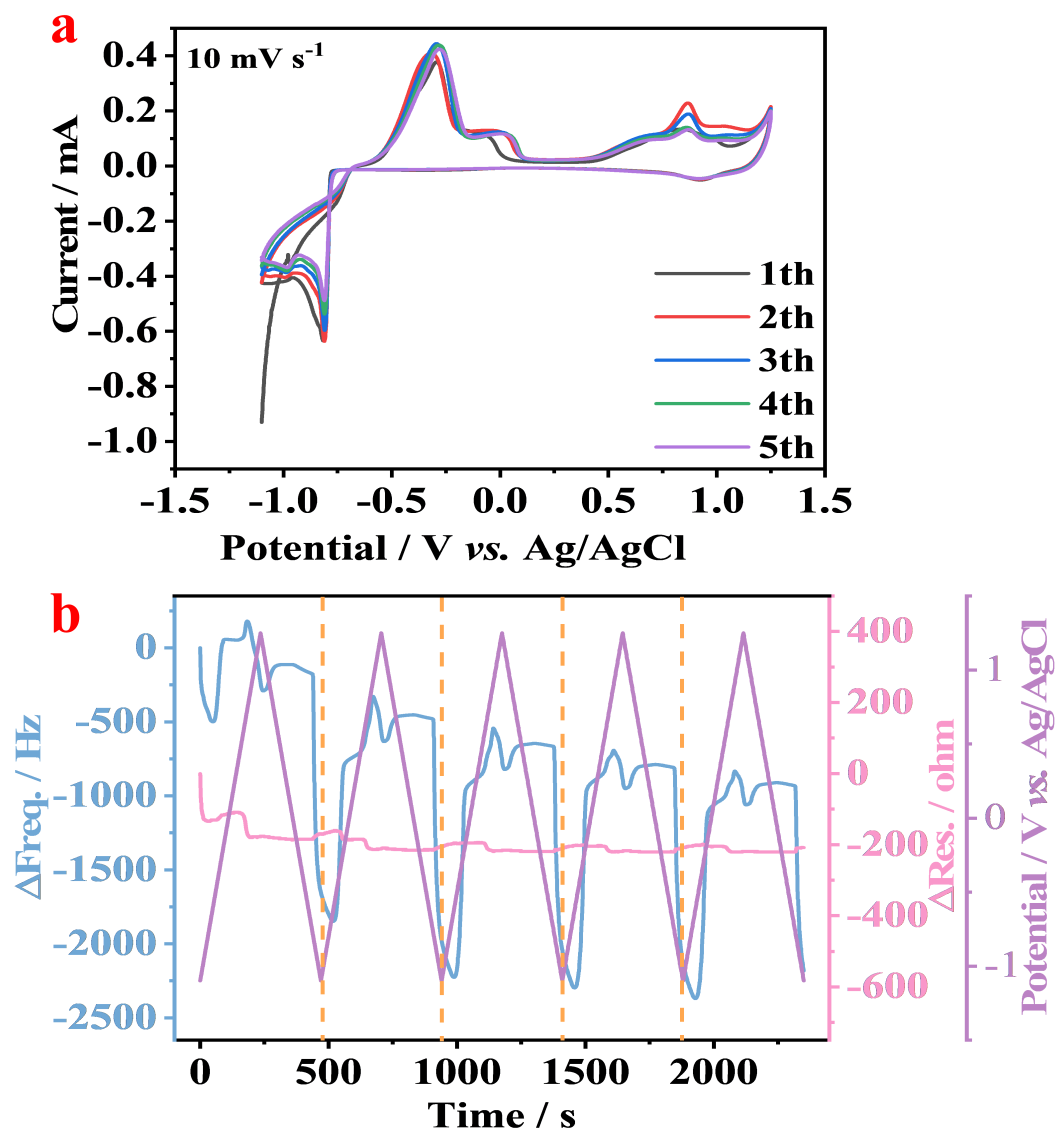


Figure S10. (a) CV curves for the first five cycles, (b) Raw EQCM data of the KCoF₃ electrode in 1 M Na₂SO₄ electrolyte (tested in the EQCM equipment).

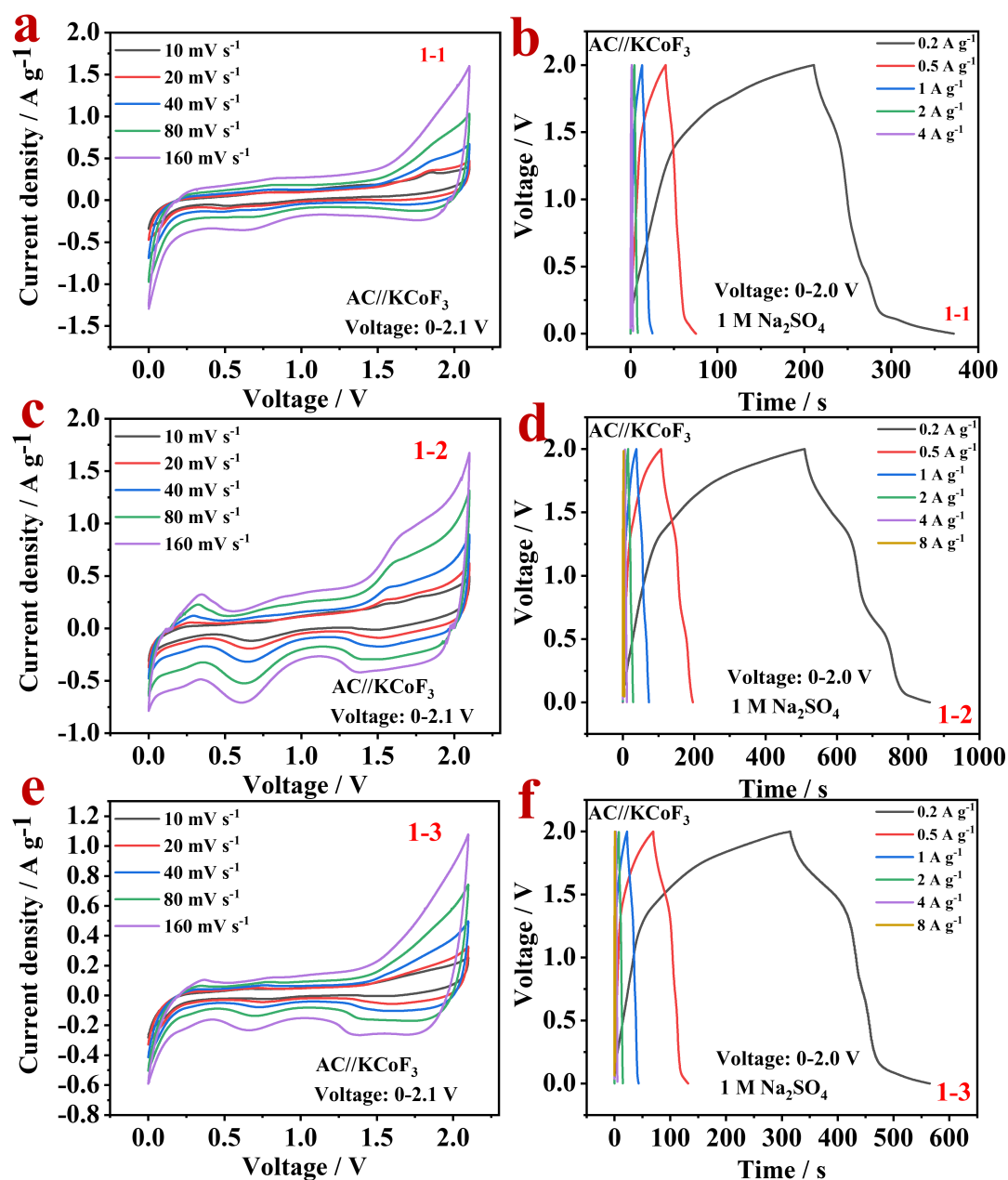


Figure S11. Aqueous ECs with positive and negative mass ratios of 1-1, 1-2, 1-3 (a, c, e) CV plots at 10~160 mV s⁻¹, (b, d, f) GCD curves at different current densities.

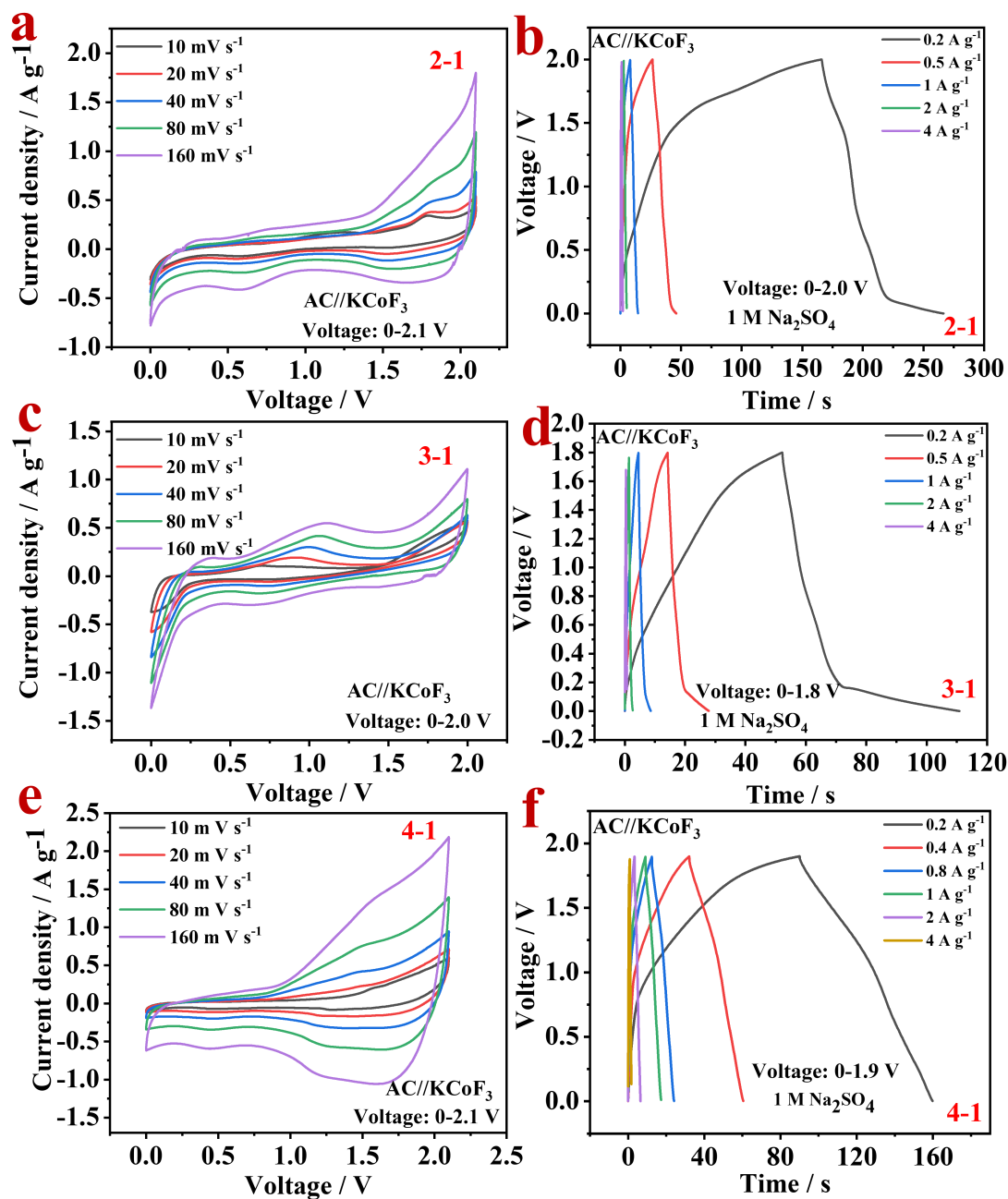


Figure S12. Aqueous ECs with positive and negative mass ratios of 2-1, 3-1, 4-1 (a, c, e) CV plots at 10~160 mV s⁻¹, (b, d, f) GCD curves at different current densities.

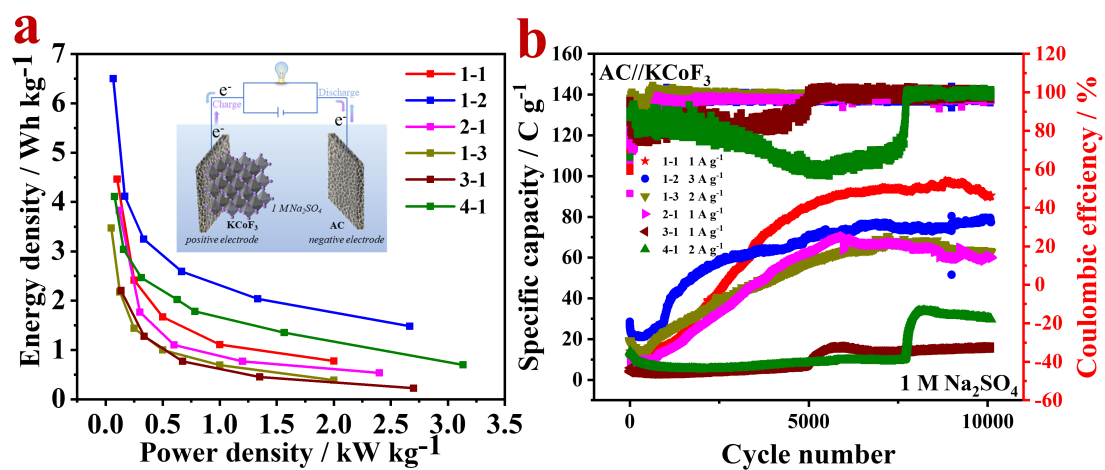


Figure S13. (a) Ragone plot (The detailed drawing for aqueous ECs structure), (b) cycling stability of aqueous ECs in different proportions.

Supplemental tables

Table S1. Materials / Chemicals used in this work.

Materials / Chemicals	Type	Company	Characteristics
CoCl ₂ ·6H ₂ O	AR	SinoPharm	Purity≥99.0%
KF·2H ₂ O	AR	SinoPharm	Purity≥99.0%
PVP-K30	GR	SinoPharm	#
Ethylene glycol (EG)	AR	SinoPharm	Purity≥99.0%
Activated carbon (Ac)	YEC-8A	Fuzhou Yihuan Carbon	Density: >0.4 g cm ⁻³ ; SSA: >2100 m ² g ⁻¹
N-Methyl pyrrolidone (NMP)	AR	Kermel	Purity≥99.0%
Poly(vinylidene fluoride) (PVDF)	Battery grade	#	#
Nickel foam	Battery grade	Tianjin Aiweixin Chemical Technology	Thickness: 1.5mm
Na ₂ SO ₄	AR	SinoPharm	Purity≥99.0%
Reference electrode (Ag/AgCl/Satd.KCl)	Ag/AgCl -6.0	Xuzhou Zhenghao Electronic Technology	Diameter: 6.0 mm
Working electrode clip (Pt)	JJ110	Shanghai Yueci Electronic Technology	10*15*0.1 mm Purity (Pt): 99.99%
Counter electrode(Pt)	#	Shanghai Three Musk Deer Industry Limited	10*10*0.2 mm Purity (Pt): 99.99%

Table S2. The EIS parameters before and after cycling for KCoF₃ electrode.

Model	Before cycling	After cycling
	$LR(Q(RW))(QR)$	$LR(QR)(QR)Q$
L (H)	5.392×10^{-19}	8.662×10^{-7}
R (Ω)	5.763	4.720
Q (S·sec ^{<i>n</i>})	2.001×10^{-4}	4.155×10^{-3}
n	0.8852	0.6930
R (Ω)	1.514×10^5	7.667
W (Y ₀ ·sec ^{0.5})	8.345×10^6	#
Q (S·sec ^{<i>n</i>})	1.135×10^{-3}	5.690×10^{-4}
n	0.632	0.7807
R (Ω)	265.4	1.041
Q (S·sec ^{<i>n</i>})	#	1.915×10^{-2}
n	#	0.6791
Chi-squared (χ^2)	7.054×10^{-4}	4.535×10^{-4}

Table S3. The crystalline parameters of the newly-formed phases in the fully charged and discharged states of KCoF₃ electrode.

Phase	PDF card	Crystal system	Space group	Cell (a×b×c) /Å
KCoF ₃	18-1006	Cubic	Pm-3m	4.0708×4.0708×4.0708
CoOOH	26-0480	Orthorhombic	Pbnm	4.353×9.402×2.84
CoO ₂	89-8399	Hexagonal	P-3m1	2.8208×2.8208×4.2403
Co ₃ O ₄	76-1802	Cubic	Fd-3m	8.072×8.072×8.072
Co(OH) ₂	74-1057	Hexagonal	P-3m1	3.173×3.173×4.64

Supplemental references

1. Y. Zhu and C. Wang, *The Journal of Physical Chemistry C*, 2010, **114**, 2830-2841.
2. W.-Y. Tsai, P.-L. Taberna and P. Simon, *J. Am. Chem. Soc.*, 2014, **136**, 8722-8728.
3. Y. Ji, Z.-W. Yin, Z. Yang, Y.-P. Deng, H. Chen, C. Lin, L. Yang, K. Yang, M. Zhang, Q. Xiao, J.-T. Li, Z. Chen, S.-G. Sun and F. Pan, *Chem. Soc. Rev.*, 2021, **50**, 10743-10763.